

Continuous critical temperature enhancement with gradual hydrogen doping in $\text{LaFeAsO}_{0.85}\text{H}_x$ ($x = 0\text{--}0.85$)

Yanfeng Guo,^{1,*} Xia Wang,^{1,2} Jun Li,^{1,2} Ying Sun,³ Yoshihiro Tsujimoto,³ Alexei A. Belik,³ Yoshitaka Matsushita,⁴ Kazunari Yamaura,^{1,2,†} and Eiji Takayama-Muromachi^{2,3}

¹*Superconducting Properties Unit, National Institute for Materials Science, 1-1 Namiki, Tsukuba, Ibaraki 305-0044, Japan*

²*Department of Chemistry, Graduate School of Science, Hokkaido University, Sapporo, Hokkaido 060-0810, Japan*

³*International Center for Materials Nanoarchitectonics (WPI-MANA), National Institute for Materials Science, Tsukuba, Ibaraki 305-0044, Japan*

⁴*NIMS Beamline Station at SPring-8, National Institute for Materials Science, 1-1-1 Kouto, Sayo-cho, Sayo-gun, Hyogo 679-5148, Japan*
(Received 9 March 2012; published 30 August 2012)

A gradual increase of the hydrogen content in $\text{LaFeAsO}_{0.85}\text{H}_x$ ($x = 0\text{--}0.85$) resulted in a continuous T_c enhancement behavior. T_c increased significantly from ~ 26 K ($x = 0$) to a value of ~ 35.5 K ($x = 0.85$). As the T_c was enhanced, structure analysis revealed a coupled gradual contraction of the lattice constants and a reduction of the As-Fe-As bond angle towards the ideal value of 109.5° of the regular tetrahedron. Since the Hall coefficient measurement detected no substantial change in the carrier number, optimization of structural parameters rather than carrier doping is likely to have played the leading role in the T_c enhancement, which could provide an important clue to the strong correlation between superconductivity and the structural parameters of iron-based superconductors. Some key phenomenological parameters, including the lower and the upper critical magnetic fields, critical current density, the density of states at the Fermi level of hydrogen-free and substituted samples, were also compared based on the magnetic and electrical characterizations, but no substantial changes were found to be associated with the hydrogen addition.

DOI: [10.1103/PhysRevB.86.054523](https://doi.org/10.1103/PhysRevB.86.054523)

PACS number(s): 74.70.Xa, 74.62.Bf, 74.62.-c, 74.25.F-

I. INTRODUCTION

Iron pnictides show superconductivity after suppression of their antiferromagnetic order,¹ through chemical substitution^{2,3} or the application of pressure,^{4,5} with a critical temperature (T_c) as high as 55 K, even rivaling doped cuprates.⁶ A striking feature of iron superconductors is that their T_c 's show a strong dependence on specific materials. For example, the maximum T_c of the so-called 1111 LnFeAsO (Ln = rare earth) system changes with diverse Ln without breaking structural symmetry, suggesting a crucial role of subtle variations in lattice parameters. More specifically, with the monotonic decrease of the lattice constant a for $\text{Ln} = \text{La} \rightarrow \text{Sm}$, T_c gets a boost from ~ 26 K to ~ 55 K,^{7,8} while a similar response was also observed in $(\text{La}, \text{Y})\text{FeAsO}_{0.6}$ (~ 20 K \rightarrow ~ 43.1 K)⁹ and $(\text{La}, \text{Na})\text{FeAsO}_{0.85}\text{F}_{0.15}$ (~ 26 K \rightarrow ~ 30.9 K)¹⁰; conversely, when a is almost saturated for $\text{Ln} = \text{Nd} \rightarrow \text{Dy}$, T_c changes only negligibly.⁷ In addition, a regular FeAs_4 tetrahedron distortion with empirical value of As-Fe-As bond angle (α) approaching 109.5° has also been found to favor a higher T_c .^{11–14} The application of pressure or isovalent substitution of P for As can also induce superconductivity, even without carrier doping.^{4,5,15} These facts indicate that the crystal structure plays at least a role similar to carrier doping in establishing the superconducting state in iron pnictides. In the five-band model, parameters including both a and α are thought to be closely related with the pnictogen height, which probably serves as the major factor affecting T_c , through controlling the multiband structure or determining the orbital fluctuations by adjusting the electron-phonon coupling strength.^{16,17} The former conjecture was experimentally proved by a recent angle-resolved photoemission spectroscopy study on $\text{PrFeAsO}_{0.7}$.¹⁸ It is notable that the

spin-fluctuations have been perceived to play an important role for the superconductivity in iron pnictides, whereas the mechanism based on the electron-phonon coupling fails to explain the superconductivity since it is too weak in this system.

Very recently, the T_c of $\text{LaFeAsO}_{0.60}$ (~ 28 K) was observed to be significantly enhanced even up to ~ 35 K by incorporation of hydrogen atoms, for example $\text{LaFeAsO}_{0.60}\text{H}_{0.60}$,¹⁹ being reminiscent of the case in $(\text{La}, \text{Y})\text{FeAsO}_{0.6}$ and $(\text{La}, \text{Na})\text{FeAsO}_{0.85}\text{F}_{0.15}$.^{9,10} Nuclear magnetic resonance (NMR) characterization indicated that hydrogen atoms in the H^- form, intercalated at the interstitial sites between the La and Fe sites, play a role in optimizing the structural parameters, possibly accounting for the T_c enhancement.²⁰ However, hydrogen incorporation in $\text{SmFeAsO}_{1-x}\text{H}_x$ ($x \sim 0.2$) induced only a comparable T_c of 55 K, with those of $\text{SmFeAs}(\text{O}, \text{F})$ or $\text{SmFeAsO}_{1-\delta}$.²¹ Thus, an indirect doping effect with hydrogen ions supplying additional electrons into the FeAs layers seems reasonable: ($\text{O}^{2-} \rightarrow \text{H}^- + \text{e}^-$) was proposed, as in the case of $\text{CeFeAsO}_{1-x}\text{H}_x$.²² However, the comparable T_c of $\text{CeFeAsO}_{1-x}\text{H}_x$ ($x = 0.25$, 48 K) and $\text{CeFeAsO}_{0.65}\text{H}_{0.65}$ (48 K) is much higher than the record created by fluorine doped $\text{CeFeAs}(\text{O}, \text{F})$ (41 K),²³ probably implying that the T_c in hydrogen-doped compounds is enhanced. Reviewing earlier reports on moisture-induced superconductivity in SrFe_2As_2 thin film ($T_c \sim 25$ K), $\text{FeTe}_{0.8}\text{S}_{0.2}$ ($T_c \sim 7.2$ K), and NaFeAs ($T_c \sim 25$ K),^{24–26} the resulting superconductivity was perceived to be produced by foreign atoms in a possible form of H_2O , OH , H , or O molecules/ions accommodated at the interstitial sites; the debate between carrier doping and structural optimization has, however, continued. Recent density functional calculations have determined that the hydrogen atoms are

stably located close to the Fe atoms at the interstitial sites, while the Fermi level was also slightly shifted upward due to band filling with hydrogen doping.²⁷ Based on the available evidences, it is hard to judge the answer to this issue at present; thus, continuous efforts aimed at yielding in-depth insights are certainly desirable.

Here we report a study of T_c enhancement in $\text{LaFeAsO}_{0.85}\text{H}_x$ ($x = 0-0.85$) with systematic hydrogen doping. The T_c increased almost linearly with the increase in hydrogen content from ~ 26 K for $x = 0$ to a final value of ~ 35.5 K for $x = 0.85$. The continuous T_c enhancement was strongly correlated with a gradual optimization of the lattice parameters upon the hydrogen incorporation, while neither the carrier number nor the superconducting parameters show any substantial change.

II. EXPERIMENTAL

The sample synthesis procedure of $\text{LaFeAsO}_{0.85}\text{H}_x$ ($x = 0.15, 0.35, 0.55, 0.70$, and 0.85) in a flat-belt-type high-pressure apparatus was similar to those reported elsewhere.^{28,29} The starting materials were laboratory-made LaAs , Fe_2O_3 (3N, Furuuchi Chem. Co.), $\text{La}(\text{OH})_3$ (3N, Wako), As (5N, High Purity Chem.), and Fe powders (3N, 100 mesh, Rare Metallic Co.). Before use, $\text{La}(\text{OH})_3$ was dried at 200°C in flowing N_2 for 3 h. Each starting mixture was sealed in a golden capsule with an h -BN (hexagonal born nitride) tube inner and then heated on the high-pressure apparatus for 2 h at an elevated temperature of 1300°C under a pressure of 6 GPa.

The phase purity of the product was examined by a powder x-ray diffraction (XRD) method in a Rigaku diffractometer (RINT2200V/PC) with $\text{Cu-K}\alpha$ radiation ($\lambda = 1.5418 \text{ \AA}$) in the 2θ range from 5° to 100° , with a step size of 2° . The structure of the samples was further investigated by a synchrotron x-ray diffraction (SXRD) method, conducted at $\lambda = 0.65298 \text{ \AA}$ in a large Debye-Scherrer camera installed on the BL15XU beam line of SPring-8.³⁰ The Rietveld analysis was carried out using the RIETAN-2000 program.³¹

Apart from hydrogen, the composition of La, Fe, and As in $\text{LaFeAsO}_{0.85}\text{H}_x$ was examined by the electron probe microanalysis (EPMA, JXA-8500F, JEOL) method, and the result is illustrated in Table I. A reliable evaluation of the exact hydrogen amount was performed by thermogravimetry and mass spectroscopy (TG-MS) in a Bruker TG-DTA 2000SA/MS 9610 apparatus, employing a similar method to that in Ref. 21. The $\text{LaFeAsO}_{0.85}\text{H}_x$ was slowly heated up to

800°C in the protection of high-purity Ar, and the evaluated hydrogen content released from each sample is also listed in Table I, normalized to the actual molar Fe content of each sample. It is clear that the evaluated values are rather close to those expected from the decomposition of $\text{LaFeAsO}_{0.85}\text{H}_{0.85}$ ($\text{LaFeAsO}_{0.85}\text{H}_x \rightarrow \text{LaFeAsO}_{0.85} + x/2\text{H}_2\uparrow$). It should be noted that the TG-MS result is the hydrogen content in the final product rather than that incorporated in the lattice of $\text{LaFeAsO}_{0.85}\text{H}_x$. The exact evaluation of hydrogen content was also accomplished with the aid of a phase purity check and EPMA analysis, which is helpful in excluding other possible hydrogen sources from impurities such as $\text{La}(\text{OH})_3$. After the evaluation of the hydrogen content, the oxygen content was also estimated with employing the similar method as that described in Ref. 29.

The direct current (dc) magnetic susceptibility (χ) was measured in a magnetic property measurement system (MPMS) from Quantum Design, under both zero-field cooling (ZFC) and field cooling (FC) conditions in a 10 Oe magnetic field between 2 and 40 K. Isothermal magnetizations at various temperatures below the T_c within the field range of ± 2 kOe were also measured using MPMS. Data on the dc electrical resistivity (ρ) were collected between 2 and 300 K with a constant gauge current of 0.2 mA in a physical properties measurement system (PPMS; Quantum Design). A four-probe method was used, with platinum wires attached to samples by silver paste. Specific heat capacity ($C_p(T)$) measurement was performed between 2 and 300 K using the same apparatus, by adopting the typical relaxation-time method. The Hall coefficient measurement in PPMS was carried out in the temperature range 50–300 K.

III. RESULTS AND DISCUSSION

First, the relation between T_c and the nominal oxygen deficiency content δ of the $\text{LaFeAsO}_{1-\delta}$ series was established. As shown in Figs. 1(a) and 1(b) by the $\rho(T)$ and the T_c vs δ , superconductivity emerges in a relatively wide window of $\delta = 0.08-0.28$, with the T_c running along a nearly dome-shaped trace with respect to δ . The dome is slightly asymmetric. Aside from the optimal point around $\delta = 0.15$, that is, in the “overdoped” regime, T_c changes relatively slowly, since superconductivity still survives at $1 - \delta = 0.72$. In the “underdoped” regime, it degenerates more rapidly, with T_c being almost completely suppressed even at $1 - \delta = 0.92$. The dome-shaped feature resembles those of other 1111- and

TABLE I. Chemical compositions analyzed for $\text{LaFeAsO}_{0.85}\text{H}_x$ ($x = 0-0.85$) (La, Fe, and As are evaluated by EPMA; H is estimated by TG-MS; O is by thermogravimetric method, as described in Ref. 29; $g(\text{O})$ is the refined result for the occupancy factor for O) and the lattice parameters.

Nominal x	La	Fe	As	O	$g(\text{O})$	H	T_c (K)	a (\AA)	c (\AA)	V (\AA^3)	α ($^\circ$)
0	1.00(2)	1.00(0)	1.00(3)	0.86(2)	0.848(5)	0(0)	26.4(4)	4.032(7)	8.713(7)	141.39(9)	113.1(4)
0.15	0.99(6)	1.00(0)	0.98(4)	0.85(4)	0.843(1)	0.14(2)	28.2(3)	4.025(3)	8.705(3)	141.05(6)	112.84(2)
0.35	1.00(1)	1.00(0)	0.99(2)	0.88(1)	0.844(2)	0.33(5)	29.5(1)	4.018(7)	8.698(6)	140.48(6)	112.47(5)
0.55	0.97(5)	1.00(0)	1.00(1)	0.86(5)	0.838(2)	0.52(3)	30.5(2)	4.012(1)	8.692(8)	139.92(6)	111.95(4)
0.70	1.00(4)	1.00(0)	0.97(6)	0.87(3)	0.852(4)	0.66(4)	32.5(1)	4.004(3)	8.688(5)	139.31(3)	111.63(6)
0.85	0.99(3)	1.00(0)	1.00(1)	0.88(2)	0.847(7)	0.82(1)	35.5(3)	4.002(6)	8.685(8)	139.15(8)	111.58(9)

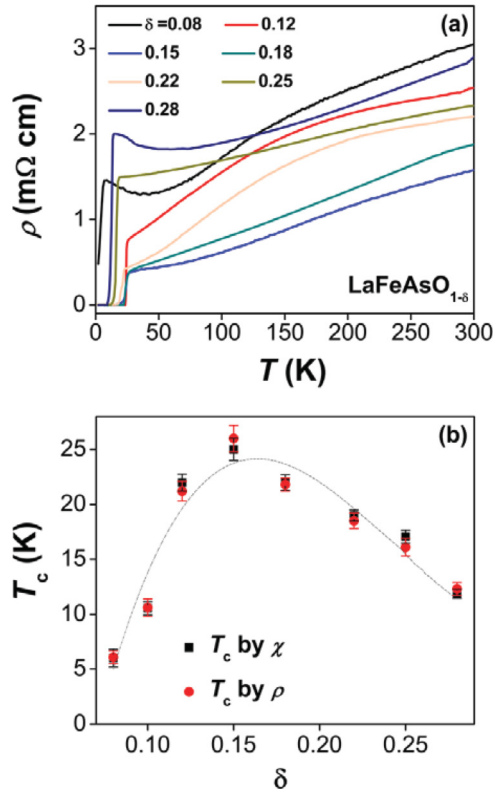


FIG. 1. (Color online) (a) The nominal oxygen deficiency content δ ($=0.08$ – 0.28) and temperature (2 – 300 K) dependence of the dc resistivity (ρ) of the polycrystalline $\text{LaFeAsO}_{1-\delta}$. The T_c exhibits a domelike feature with respect to δ , as shown in (b).

122-type doped superconductors, such as $\text{TbFeAsO}_{1-\delta}$, $\text{NdFe}_{1-x}\text{Co}_x\text{AsO}$, and $\text{Ba}(\text{Fe}, TM)_2\text{As}_2$ (TM = transition metals).^{32–35} Provided that carrier doping is the simple source for the introduction of superconductivity, T_c will be driven into the “overdoped” regime and hence will suffer a reduction when more carriers are added into the “optimal” $\text{LaFeAsO}_{0.85}$, as occurs in cuprate superconductors.

The room temperature XRD characterization on $\text{LaFeAsO}_{0.85}\text{H}_x$ ($x = 0, 0.15, 0.35, 0.55, 0.70$, and 0.85) indicates that all specimens studied herein hold the same crystal symmetry, adopting a tetragonal unit cell (space group: $P4/nmm$) with a ZrCuSiAs -type structure.³⁶ The structural details will be discussed later. To document the effect of H addition on the T_c of $\text{LaFeAsO}_{0.85}$, $\chi(T)$ and $\rho(T)$ of $\text{LaFeAsO}_{0.85}\text{H}_x$ are shown in Figs. 2(a)–2(f) and 2(g)–2(l), respectively. For hydrogen-free $\text{LaFeAsO}_{0.85}$, a sharp drop of χ at $T_c \sim 25$ K (derived from $d\chi/dT$) is visible, corresponding to the onset temperature of diamagnetism; this is comparable with previous reports.²⁹ The diamagnetic shielding fraction at 2 K was estimated to be 0.94, based on the calculated density of 6.667 g/cm³, provided that the perfect diamagnetism is 1.00, thus ensuring bulk superconductivity. Once an appropriate amount of hydrogen is introduced when the oxygen content is fixed at $1 - \delta = 0.85$, the effect is immediately manifested by the progressively raised T_c , which increases almost linearly as hydrogen addition progresses, from 25 K at $x = 0$ finally to 35 K at $x = 0.85$, as indicated by the T_c of χ . The magnitude of the increase (10 K) is slightly larger than that

reported for $\text{LaFeAsO}_{0.60}$ in Ref. 19 (28 K \rightarrow 35 K). Our results not only confirm that T_c can be enhanced but also reveal that it can be continuously increased with the gradual incorporation of the hydrogen content. The same result can also be observed from the $\rho(T)$ shown in Figs. 2(g)–2(l). From the enlarged part between 2 and 40 K inserted in each figure, it is clear that even the magnitude of the T_c enhancement is comparable with that derived from $\chi(T)$, despite the slightly larger T_c of $\rho(T)$ for $x = 0.85$, 35.5 K, suggesting that the result is highly reproducible. Moreover, in the normal state, neither the magnitude nor the characteristics of $\rho(T)$ change remarkably. Taking the $T_c - \delta$ phase diagram of $\text{LaFeAsO}_{1-\delta}$ into account, the role of hydrogen addition as carrier doping probably cannot account for the T_c enhancement of “optimal” $\text{LaFeAsO}_{0.85}$, differing significantly from what it does during the establishment of the superconducting states in SmFeAsO ,²¹ undoped SrFe_2As_2 film,²⁴ and other analogous cases.

To further guarantee the bulk superconductivity, as well as to probe the quasiparticle density of states (DOS) at the Fermi level (E_F), the specific heat of $\text{LaFeAsO}_{0.85}\text{H}_x$ was presented. The low temperature parts in the form of $C_p(T)/T$ vs T for $\text{LaFeAsO}_{0.85}$ and $\text{LaFeAsO}_{0.85}\text{H}_{0.85}$ between 2 and 40 K are summarized in Figs. 3(a) and 3(b) as examples, with the expected thermodynamic anomalies that signaled the superconducting transitions being visible at 25 K and 35.5 K, suggesting that the polycrystals are in inhomogeneous superconducting state. The lattice contribution was accurately extracted by a method similar to that in Ref. 37, using $\text{LaFe}_{0.9}\text{Mn}_{0.1}\text{AsO}_{0.85}$ as the initial compound. Here, the superconductivity is sufficiently suppressed without resulting in other magnetic anomalies—including the Schottky anomaly—in any magnetic field; thus it will not harm the extraction. The C_p for $\text{LaFe}_{0.9}\text{Mn}_{0.1}\text{AsO}_{0.85}$ is shown in Fig. 3(c), and its presentation in the C_p/T vs T^2 form as an inset is indeed magnetic field independent. The fit to low-temperature data yielded the electronic contribution term γ_n^{Mn} as $1.68(3)$ mJ/mol K². The lattice contribution of $\text{LaFe}_{0.9}\text{Mn}_{0.1}\text{AsO}_{0.85}$, $C_{\text{latt}}^{\text{Mn}}$, was consequently obtained by subtracting $\gamma_n^{\text{Mn}}T$ from the total C_p . Due to the slight differences of the lattice parameters between $\text{LaFe}_{0.9}\text{Mn}_{0.1}\text{AsO}_{0.85}$ and $\text{LaFeAsO}_{0.85}\text{H}_x$, we thus can assume that the phonon contribution to the $C_p(T)$ and to entropy obey the law of corresponding states, hence the normal-state of C_p of $\text{LaFeAsO}_{0.85}\text{H}_x$ can be obtained from the corresponding states approximation with the formula^{37,38}

$$C_{\text{tot}}(T) = C_{\text{latt}}(T) + \gamma_n T = AC_{\text{latt}}^{\text{Mn}}(BT) + \gamma_n T, \quad (1)$$

where γ_n is the Sommerfeld constant of $\text{LaFeAsO}_{0.85}\text{H}_x$ in the normal state, and A and B are plotted constants (listed in Table II). The difference between the measured $C_p(T)/T$ and the normal-state counterpart $C_{\text{latt}}(T)/T$, $\Delta C_{\text{el}}(T)/T$, was inserted in each corresponding figure, revealing clear jumps at $T_c = 25.1(2)$ K and $35.5(5)$ K (corresponding to the T_c of $\text{LaFeAsO}_{0.85}$ and $\text{LaFeAsO}_{0.85}\text{H}_{0.85}$, respectively), thus providing compelling evidence for bulk superconductivity. The close values of γ_n for $\text{LaFeAsO}_{0.85}$ and $\text{LaFeAsO}_{0.85}\text{H}_{0.85}$, 1.65 and 1.71 mJ/mol K², both agree well to those values for $\text{LaFeAsO}_{1-\delta}$, Co- and F-doped LaFeAsO .^{29,39,40} The estimation of the electronic DOS at the Fermi level ($N(E_F)$)

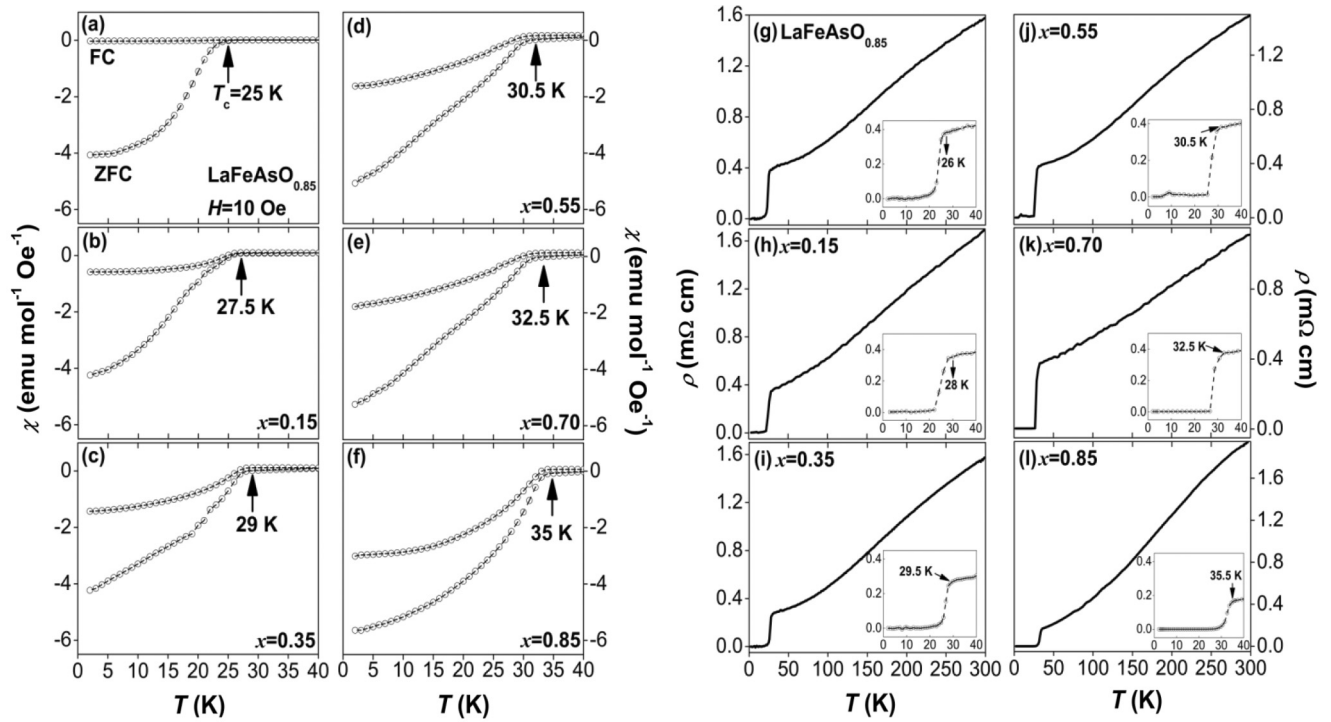


FIG. 2. (a)–(f) The dc magnetic susceptibilities $\chi(T)$ (2–40 K) for $\text{LaFeAsO}_{0.85}\text{H}_x$ ($x = 0$ –0.85) with the transition temperature being marked. (g)–(l) The resistivity $\rho(T)$ (2–300 K) for each sample and the corresponding insets enlarge the low temperature part between 2–40 K.

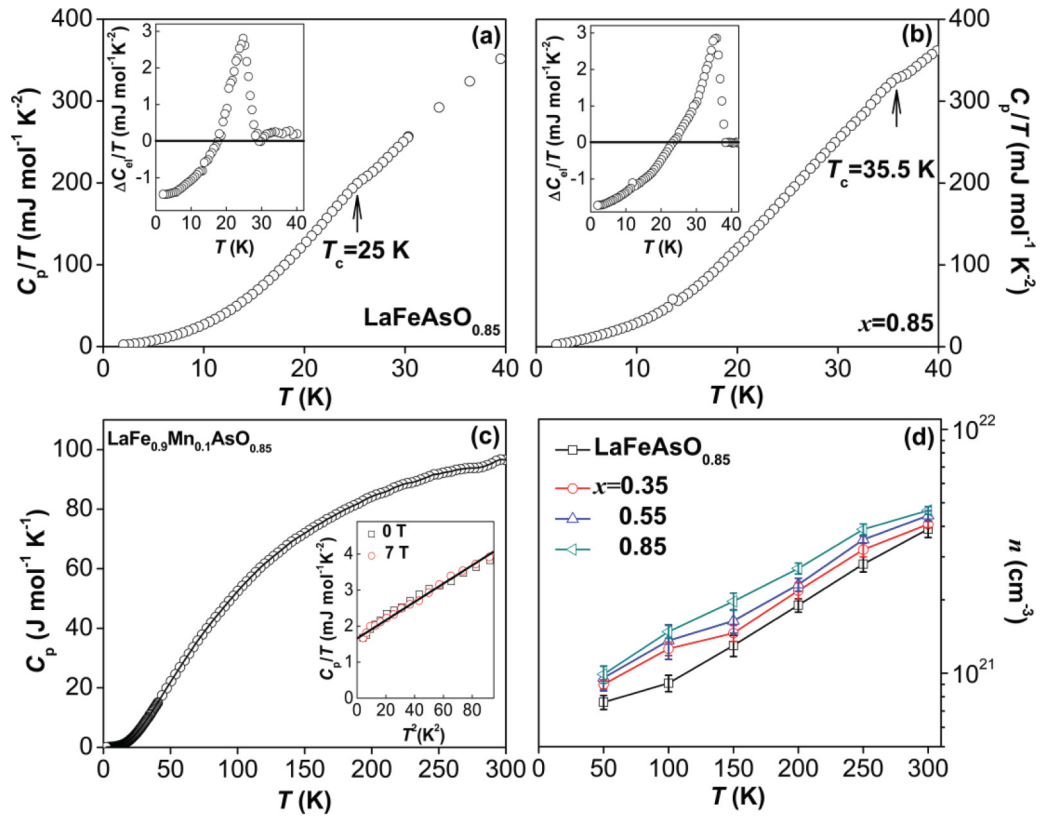


FIG. 3. (Color online) (a) and (b) The specific heat in the form C_p/T vs T for $\text{LaFeAsO}_{0.85}$ and $\text{LaFeAsO}_{0.85}\text{H}_{0.85}$ between 2–40 K, and the corresponding insets present the difference between the measured $C_p(T)/T$ and the normal-state counterpart $C_{\text{lat}}(T)/T$. The main panel of (c) shows the specific heat for $\text{LaFe}_{0.9}\text{Mn}_{0.1}\text{AsO}_{0.85}$, and the low temperature part in the form C_p/T vs T^2 shows field independence and no other anomalies. (d) The temperature dependence of carrier density n of $\text{LaFeAsO}_{0.85}\text{H}_x$ ($x = 0$ –0.85).

TABLE II. Scale factors A and B , γ , $N(E_F)$, $H_{c1}(0)$, and $H_{c2}(0)$ of $\text{LaFeAsO}_{0.85}\text{H}_x$ ($x = 0-0.85$).

x	A	B	γ (mJ mol ⁻¹ K ²)	$T_c(C_p)$ (K)	$N(E_F)$ (states eV ⁻¹ f.u. ⁻¹)	n (10 ²¹ cm ⁻³)	$H_{c2}(0)$ (T)	$H_{c1}(0)$ (10 ⁻³ T)
0.00	0.97	1.04	1.65(1)	25.1(2)	0.993(7)	3.92(3)	35.0(4)	6.28(9)
0.15	0.99	1.01	1.63(3)	27.5(4)	0.983(4)	4.01(5)	33.6(2)	6.19(1)
0.35	0.98	1.04	1.66(1)	29.2(4)	0.999(5)	3.97(13)	31.5(1)	6.09(3)
0.55	1.02	1.05	1.64(5)	30.5(2)	0.988(2)	4.12(2)	31.9(3)	5.97(4)
0.70	0.95	1.02	1.67(3)	32.7(4)	1.004(6)	4.18(4)	30.2(5)	5.91(3)
0.85	1.01	0.98	1.69(2)	35.5(5)	1.014(8)	4.29(2)	32.7(1)	5.87(7)

with the aid of γ_n gave values around 1 states/eV per unit cell for the $\text{LaFeAsO}_{0.85}\text{H}_x$ series from the relation $\gamma_n = \frac{\pi^2}{3} k_B^2 N(E_F)(1 + \lambda_{ep})$ by assuming $\lambda_{ep} = 0$, since the electron-phonon coupling is very weak.⁴¹ By idealizing the $C_p(T)$ anomaly under the constraint of entropy balance between the superconducting and normal state as $\int_0^{T_c} (c_e(T)) dT = \gamma_n T_c$, the accurate determination of $T_c(C_p)$ was accomplished (in Table II). Throughout the listed values in Table II, $N(E_F)$ actually changes negligibly over the hydrogen concentrations, while $T_c(C_p)$ changes in a comparable way to those identified by both $\chi(T)$ and $\rho(T)$, making it probable that hydrogen addition plays a minor role in providing carriers into $\text{LaFeAsO}_{0.85}$. Further evidence was obtained by the evaluation of the carrier density shown in Fig. 3(d), calculated from the measured Hall coefficient. The profiles of all studied specimens are very similar, indicating little change of the electron number over the hydrogen addition. The carrier density at 300 K for $\text{LaFeAsO}_{0.85}\text{H}_x$ was $3.92(3) \times 10^{21} \text{ cm}^{-3}$ – $4.29(2) \times 10^{21} \text{ cm}^{-3}$ (shown in Table II), corresponding to about 1.1 electrons per primitive cell, being also comparable with the values reported for F-doped LaFeAsO .⁴² Even with further cooling, the difference in carrier density among independent samples was actually very small.

The $\rho(T)$ for $\text{LaFeAsO}_{0.85}$ and $\text{LaFeAsO}_{0.85}\text{H}_{0.85}$ in various magnetic fields H is depicted in Figs. 4(a) and 4(b), respectively. H markedly pushes the zero-resistance temperature T_{c0} from 21.3 K at $H = 0$ T to 14.5 K at $H = 9$ T of $\text{LaFeAsO}_{0.85}$. The criteria of a 10%, 50%, and 90% drop of $\rho(T)$ across the superconducting transition were adopted for the evaluations, which are shown as insets in Figs. 4(a) and 4(b). The initial slopes yielded in the vicinity of T_c , $\partial H_{c2}/\partial T$, are about -0.387 T/K, -0.25 T/K, and -0.245 T/K, respectively. Since the 90% criterion is generally harmed by the vortex-liquid phase, while the 10% criterion tends to be disturbed by the superconducting fluctuations,^{43–46} the ground state value $H_{c2}(0)$ is about 35.0(4) T, fitting the 50% criterion to the Werthamer-Helfand-Hohenberg (WHH) relation (shown by the solid line) $\mu_0 H_{c2}(T) = -0.693 \mu_0 (dH_{c2}/dT)_{T=T_c} T_c$ and neglecting the effect from spin paramagnetism ($\alpha = 0$) and spin-orbit scattering ($\lambda_{SO} = 0$).⁴⁷ The value is smaller than those of $\text{NdFe}_{1-x}\text{Rh}_x\text{AsO}$ (10^2 T)⁴⁸ and $\text{LaFeAsO}_{0.89}\text{F}_{0.11}$ (45 T).⁴⁹ For $\text{LaFeAsO}_{0.85}\text{H}_{0.85}$, H sharply reduces the T_{c0} from 29.6 K at $H = 0$ T to $T_{c0} = 15.6$ K at 9 T, thus giving rise to $\partial H_{c2}/\partial T \approx -0.22$ T/K and $H_{c2}(0) = 32.7(1)$ T, using the 50% criterion. The slight difference between the $H_{c2}(0)$

of $\text{LaFeAsO}_{0.85}$ and $\text{LaFeAsO}_{0.85}\text{H}_{0.85}$ indicates a moderate effect from hydrogen addition. Provided the evaluation is close to the truth, the $H_{c2}(0)$ values of both samples are smaller than the weak-coupling estimation of the BCS paramagnetic critical field, $\mu_0 H_P = 1.84 T_c \sim 44$ T, possibly suggesting the orbital effect plays the dominant role. Assuming that H_{c2} is purely orbital, the coherence length ξ_{GL} at $T = 0$ can be estimated from the single-band Ginzburg-Landau relation $\xi_{GL} = \sqrt{\phi_0/2\pi H_{c2}(0)}$, where ϕ_0 is the flux quantum, giving $\xi_{GL}(0) = 30.6(6)$ Å for $\text{LaFeAsO}_{0.85}$ and 31.7(4) Å for $\text{LaFeAsO}_{0.85}\text{H}_{0.85}$, respectively, suggesting little change with the hydrogen substitution.

In addition to gradually raising the T_c , the hydrogen addition also enhances the Meissner fractions in the $\chi(T)$ curves. This can be clearly seen by the FC curves in Figs. 2(a)–2(f) of $\text{LaFeAsO}_{0.85}\text{H}_x$, in which the absolute

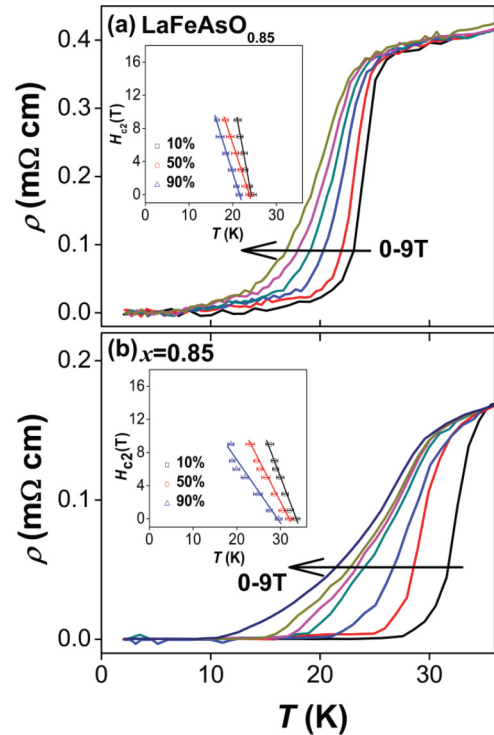


FIG. 4. (Color online) Temperature and field ($H = 0, 1, 3, 5, 6, 7$, and 9 T) dependence of the resistivity of polycrystalline (a) $\text{LaFeAsO}_{0.85}$ and (b) $\text{LaFeAsO}_{0.85}\text{H}_{0.85}$. The inset in each figure presents the upper critical field H_{c2} found from 90%, 50%, and 10% of the superconducting drop.

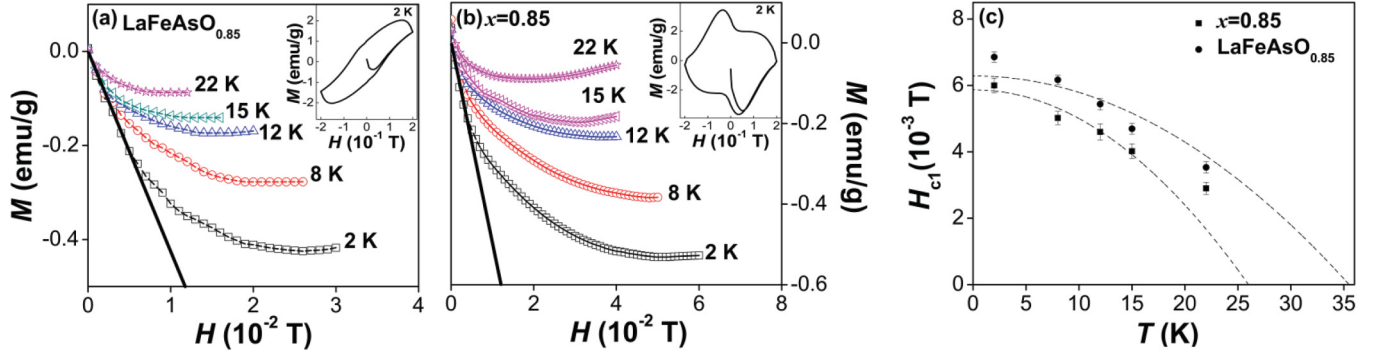


FIG. 5. (Color online) Low field $M(H)$ of (a) $\text{LaFeAsO}_{0.85}$ and (b) $\text{LaFeAsO}_{0.85}\text{H}_{0.85}$ at various temperatures. The insets in each figure show the $M(H)$ loops up to 0.2 T. The solid line is drawn to show the linear part of the data measured at 2 K. (c) The temperature dependence of $H_{c1}(T)$; the dotted lines are fit to the data with the formula $H_{c1}(T) = H_{c1}(0)(1 - t^2)$, where t is defined as $t = T/T_c$.

values of the magnetic moments except in the vicinity of T_c apparently increase. The Meissner fraction of $\text{LaFeAsO}_{0.85}$ is fairly small, less than 0.1, as was estimated by using the FC data at 2 K. Such contrasting features between the magnetic shielding and the Meissner fractions have been commonly observed in oxygen-deficient 1111 systems³² and are probably due to efficient magnetic-flux pins and a small particle size that is not far from the magnetic penetration depth ($\sim 0.25 \mu\text{m}$ ⁵⁰). In $\text{LaFeAsO}_{0.85}\text{H}_{0.85}$ the Meissner fraction increases significantly, even up to ~ 0.4 (FC, 5 K). This behavior would be interesting to study further. Meanwhile, the magnetization isotherms of $\text{LaFeAsO}_{0.85}$ and $\text{LaFeAsO}_{0.85}\text{H}_{0.85}$, presented as insets in Figs. 5(a) and 5(b), exhibit typical behavior of a type-II superconductor. The $M(H)$ profiles of the two samples are different even at a first glance. The lower critical field (H_{c1}) at which the magnetization deviates from a linear response is identified. A least-squares fit to the data using $H_{c1}(T) = H_{c1}(0)(1 - t^2)$ (the $t = T/T_c$) yielded the ground state values of $\text{LaFeAsO}_{0.85}$ and $\text{LaFeAsO}_{0.85}\text{H}_{0.85}$ as $H_{c1}(0) = 6.28(6) \times 10^{-3}$ T and $5.87(7) \times 10^{-3}$ T, respectively [Fig. 5(c)].⁵¹ The $H_{c1}(0)$ leads to a London penetration depth $\lambda(0)$ of 3.18×10^3 Å for $\text{LaFeAsO}_{0.85}$ and 3.22×10^3 Å for $\text{LaFeAsO}_{0.85}\text{H}_{0.85}$, respectively, through the Bardeen-Cooper-Schrieffer formula $H_{c1}(T) = (\phi_0/4\pi\lambda^2) \ln(\lambda/\xi_{\text{GL}})$. We also estimated J_c by applying the Bean model with the formula $J_c = 20\Delta M/Va(1 - 2a/3b)$,⁵² where ΔM is the width of the M - H loop, and V , a , and b are the volume, width, and length of the polycrystal, respectively. The estimated J_c at 2 K of $\text{LaFeAsO}_{0.85}\text{H}_{0.85}$ is about 5200 A/cm², being far lower than those reported for the 122-system, suggesting a prominent grain boundary effect where the grains are somewhat weakly linked as compared to single crystals.^{53,54} Exceptionally, hydrogen addition does not substantially enhance J_c despite the T_c being slightly raised: 4500 A/cm² for $\text{LaFeAsO}_{0.85}\text{H}_{0.85}$ at 2 K.

The relation between T_c and lattice parameters of the $\text{LaFeAsO}_{1-\delta}$ series resembles those previously established, for example, for $\text{TbFeAsO}_{1-\delta}$.³² Lattice constants of a , b , and the unit-cell volume (V) of $\text{LaFeAsO}_{1-\delta}$ are illustrated in Figs. 6(a)–6(c). The parameters show a similar evolution trend, reaching the minimal value, while T_c is optimized at $\delta = 0.15$ and then rising again with the increase of δ

into the “overdoped” regime. The tight correlation between T_c (by ρ) and lattice constant a is shown in Fig. 6(d), revealing that a higher T_c appears at a smaller a . However, the refined As-Fe-As bond angle, even at $\delta = 0.15$, is as large as $113.09(9)^\circ$, indicating that the local distortion of the FeAs_4 tetrahedron deviates significantly from a regular state with the empirical value of 109.5° , as illustrated by Fig. 6(e); hence, the T_c of 26 K is much lower than the record of ~ 55 K for an Sm-based 1111 superconductor with As-Fe-As bond angle 109.76° and a constant $3.90236(8)$ Å.⁵⁵ The T_c value is also slightly lower than that of $\text{LaFeAsO}_{0.60}$ synthesized under a pressure of 3 GPa (~ 28 K), whose structure parameters are slightly improved.⁷ This fact implies that a further optimization of the crystal structure of the $\text{LaFeAsO}_{1-\delta}$ can yield a higher T_c , as in the case of hydrogen doping.

The Rietveld analysis result of $\text{LaFeAsO}_{0.85}$ was already presented in Ref. 29. Figure 6(f) shows the observed, calculated, and difference profiles of $\text{LaFeAsO}_{0.85}\text{H}_{0.85}$ as an example. The SXRD pattern can be satisfactorily reproduced by the ZrCuSiAs -type structure model with the lattice parameters $a = 0.400166(10)$ Å and $c = 0.86858(2)$ Å. The reliability indices ($R_{\text{wp}} = 3.185\%$, $R_p = 2.166\%$, and $R_F = 0.362\%$) are sufficiently low, indicating the high quality of the fit, as does a comparison between the refined and the experimental patterns. The structure solutions are listed in Table III compared with those of $\text{LaFeAsO}_{0.85}$. The analysis revealed 0.72 mass% of $\text{La}(\text{OH})_3$, 0.43 mass% of LaAs , 1 mass% of La_2O_3 , and 1.34 mass% of Fe. The tiny amount of $\text{La}(\text{OH})_3$ indicates that the exact content of hydrogen in $\text{LaFeAsO}_{0.85}\text{H}_{0.85}$ is close to the nominal value. Several main peaks (102), (110), and (111) of the powder XRD patterns of $\text{LaFeAsO}_{0.85}\text{H}_x$ are inserted in Fig. 6(f) as examples to show the evolution trend upon hydrogen doping, which exhibits a systematic shift with the increase of hydrogen content. The change is clearly shown by the lattice parameters summarized in Table I, including a , c , V , and As-Fe-As, which show a monotonic decrease with the increase of hydrogen level, suggesting that hydrogen addition slightly compresses the unit cell; the changes of $\text{LaFeAsO}_{0.85}\text{H}_{0.85}$ from those of the host $\text{LaFeAsO}_{0.85}$ are approximately 0.746% for a , 0.32% for c , 1.585% for V , and 1.37% for As-Fe-As. The results also imply the successful

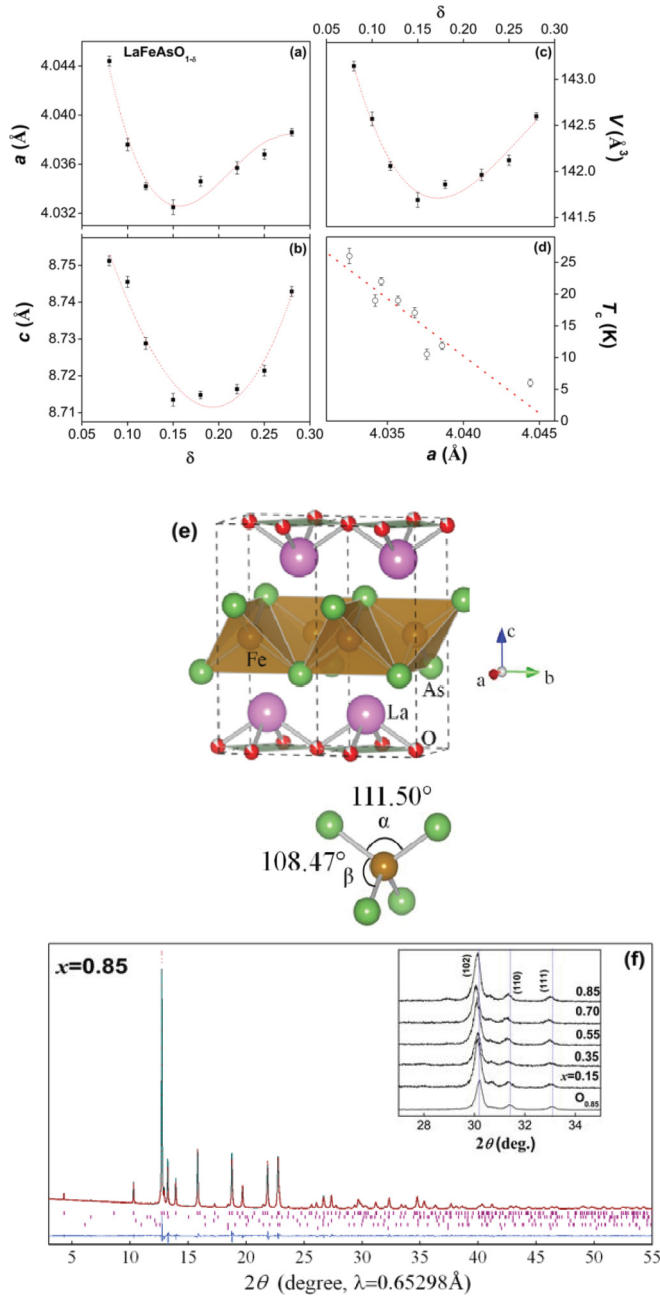


FIG. 6. (Color online) (a)–(c) a , c , and the volume of the tetragonal unit cell evolution through oxygen quantity of $\text{LaFeAsO}_{1-\delta}$, respectively. (d) T_c vs the a -axis parameter for $\text{LaFeAsO}_{1-\delta}$. (e) A structural view of $\text{LaFeAsO}_{0.85}\text{H}_x$, drawn based on the refined results, and (f) the Rietveld analysis results of synchrotron x-ray profiles of $\text{LaFeAsO}_{0.85}\text{H}_{0.85}$. Cross markers and solid lines show the observed and calculated profiles, respectively. The difference curve is at the bottom of each. The positions of Bragg reflections are marked by ticks. Center and bottom lines of ticks are for the impurities $\text{La}(\text{OH})_3$ (0.72%), LaAs (0.43%), La_2O_3 (1%), and Fe (1.34%), respectively, with the weight fractions marked in each bracket. Insets show the evolution of several major peaks of $\text{LaFeAsO}_{0.85}\text{H}_x$ measured at $\lambda = 1.5418 \text{ \AA}$.

incorporation of hydrogen to at least above $x = 0.70$ without touching the solubility limit. The continuous decrease of lattice

TABLE III. Structure parameters of $\text{LaFeAsO}_{0.85}$ (top) and $\text{LaFeAsO}_{0.85}\text{H}_{0.85}$ (bottom) determined by a synchrotron x-ray powder diffraction data ($\lambda = 0.65298 \text{ \AA}$) at room temperature. Space group is $P4/nmm$ (no. 129) at origin choice 2, $Z = 2$. R factors were $R_{\text{wp}} = 3.82\%$, $R_p = 2.56\%$, and $R_F = 3.08\%$ for $\text{LaFeAsO}_{0.85}$; $R_{\text{wp}} = 3.185\%$, $R_p = 2.166\%$, and $R_F = 0.362\%$ for $\text{LaFeAsO}_{0.85}\text{H}_{0.85}$. Selected bond lengths (d) and angles are $d_{\text{Fe-As}} = 2.4168(6) \text{ \AA} (\times 4)$, $d_{\text{La-O}} = 2.3741(3) \text{ \AA} (\times 4)$, $\alpha_{\text{As-Fe-As}} = 113.1(4)^\circ$, $72.34(5)^\circ$ for $\text{LaFeAsO}_{0.85}$; and $d_{\text{Fe-As}} = 2.4206(4) \text{ \AA} (\times 4)$, $d_{\text{La-O}} = 2.3902(3) \text{ \AA} (\times 4)$, $\alpha_{\text{As-Fe-As}} = 111.58(9)^\circ$, $71.66(9)^\circ$ for $\text{LaFeAsO}_{0.85}\text{H}_{0.85}$.

Site	Wyckoff position	g	x	y	z	$B (\text{\AA}^2)$
La	$2c$	1	0.25	0.25	0.14364(10)	0.62(2)
Fe	$2b$	1	0.75	0.25	0.5	0.73(1)
As	$2c$	1	0.25	0.25	0.65289(17)	0.78(4)
O	$2a$	0.848(5)	0.75	0.25	0	0.53(2)
La	$2c$	1	0.25	0.25	0.15119(5)	0.57(1)
Fe	$2b$	1	0.75	0.25	0.5	0.58(2)
As	$2c$	1	0.25	0.25	0.65607(8)	0.72(1)
O	$2a$	0.847(7)	0.75	0.25	0	1.5(2)

parameters with the hydrogen addition resembles the case of applying pressure,⁵⁶ which more markedly reduces the lattice parameters approximately 4.3% for a , 9.86% for c , and 17.4% for V when the applied pressure reaches 32.26 GPa. Because the x-ray atomic scattering factor of hydrogen is too small, it is hard to refine either its site position or the occupancy. During the Rietveld analysis, the values of the temperature factors, U_{iso} , for La, Fe, As, and O were initially fixed as those in the undoped sample, then the occupancy factor of O was also refined.

Regarding the contraction of the lattice constants, three possibilities have been proposed.^{19,20,22} The first is that the incorporated hydrogen is in a H^+ form located at the interstitial site between La and Fe sites, thus attracting the neighboring O^{2-} and/or As^{3-} ions.¹⁸ The second is that hydrogen is in an H^- (1.275 \AA) form at the O^{2-} (1.42 \AA) site,^{20,22} which then results in electron doping in the FeAs layer, thus attracting two layers much closer; this is possibly supported by the fact of the reduced Fe-Fe distance from 2.8514(1) \AA of $\text{LaFeAsO}_{0.85}$ to 2.8294(1) \AA of $\text{LaFeAsO}_{0.85}\text{H}_{0.85}$. The final possibility is that the O^{2-} ions are replaced by the $(\text{OH})^-$ ions, and the slight difference between their ionic size (1.40 \AA for O^{2-} and 1.37 \AA for $(\text{OH})^-$) leads to the contraction of the unit cell.²⁰ However, taking the domelike relation between T_c and δ into account, overcharge doping in the optimal $\text{LaFeAsO}_{0.85}$ superconductor will decrease the T_c , which is not consistent with our observations.

A natural question is why the effects on $\text{LaFeAsO}_{1-\delta}$, CeFeAsO and SmFeAsO associated with hydrogen doping are so different? The T_c of $\text{LaFeAsO}_{0.85}$, $\text{LaFeAsO}_{0.60}$, and CeFeAsO increases beyond the records created by carrier doping either by oxygen deficiency or fluorine doping, whereas the T_c produced in $\text{SmFeAsO}(\text{O},\text{H})$ is only comparable with that of a doped sample of 55 K.²¹ In fact, the effort by hydrogen doping also failed to raise the T_c in $\text{SmFeAsO}_{0.60}\text{H}_{0.60}$.⁵⁷ One fact that must be taken into account is that the structure of the Sm-1111

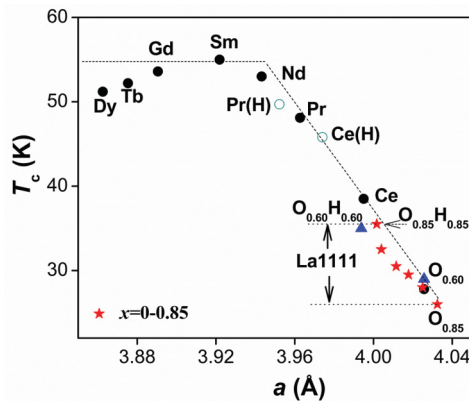


FIG. 7. (Color online) Relationship between the a -axis parameter and T_c of $\text{LaFeAsO}_{0.85}\text{H}_x$ and $\text{LnFeAsO}_{1-\delta}$ ($\text{Ln} = \text{La}, \text{Dy}, \text{Tb}, \text{Gd}, \text{Sm}, \text{Nd}, \text{Pr}, \text{and Ce}$). The a parameters, except for $\text{LaFeAsO}_{0.85}\text{H}_x$, are obtained from Refs. 7, 8, 19, and 20.

system is almost optimized; it is rather difficult to improve it further through hydrogen doping. In contrast, the parameters of La-1111 and Ce-1111 systems are far from being optimized; thus, hydrogen doping can precisely play that role. On the other hand, taking into account the relation between T_c and the lattice constant a of some 1111 superconductors, as presented in Fig. 7, the values of a of the hydrogen-doped $\text{LaFeAsO}_{0.85}$, as well as other key parameters such as As-Fe-As bond angle, are located between Ce-1111 ($T_c = 38.5$ K, $a = 0.3995$ nm)⁷ and $\text{LaFeAsO}_{0.85}$; hence their T_c are just between them. For all the lattice parameters listed in Table III, the evolution tendency of the FeAs_4 tetrahedron of $\text{LaFeAsO}_{0.85}\text{H}_x$ with the increase of hydrogen incorporation is apparently toward an ideal distortion state, indicative of clear structural optimization behavior.

In summary, the hydrogen addition in $\text{LaFeAsO}_{0.85}$ was realized under high-pressure conditions, which remarkably raises the critical temperature T_c from 26 K gradually up to ~ 35.5 K. The nearly linearly increase of T_c with the hydrogen content was found to be associated with a gradual optimization of lattice parameters, without substantially changing the carrier concentrations, probably suggesting that optimization of structural parameters rather than carrier doping is the major reason. It is clearly consistent with the opinion in Ref. 16 for interpreting the T_c enhancement in $\text{LaFeAsO}_{0.60}\text{H}_{0.60}$ rather than a carrier doping effect proposed in Refs. 21 and 22 for both $\text{SmFeAs}(\text{O},\text{H})$ and $\text{CeFeAs}(\text{O},\text{H})$.^{21,22} Since there is a debate between carrier doping and structure tuning as the source for superconductivity in iron pnictides, it has been difficult to establish a solid picture as was done for cuprate superconductors. The results reported herein provide helpful supporting data and clues to the study. It could also be interesting to study how the magnetic excitations/fluctuations with hydrogen-addition in such 1111 families evolve, since the substitution seems to be involved in the superconductivity mechanism. Moreover, the results could indicate an effective direction in the search for new superconductors with a high T_c by focusing on structural design.

ACKNOWLEDGMENTS

This research was supported in part by the World Premier International Research Center from MEXT, Grants-in-Aid for Scientific Research (22246083) from JSPS, the Funding Program for World-Leading Innovative R&D on Science and Technology (FIRST Program) from JSPS, and the Advanced Low Carbon Technology Research and Development Program (ALCA) from JST.

*guo.yanfeng@nims.go.jp

†Yamaura.Kazunari@nims.go.jp

¹C. de la Cruz, Q. Huang, J. W. Lynn, J. Y. Li, W. Latcliff, II, J. L. Zarestky, H. A. Mook, G. F. Chen, J. L. Luo, N. L. Wang, and P. C. Dai, *Nature (London)* **453**, 899 (2008).

²M. Rotter, M. Tegel, and D. Johrendt, *Phys. Rev. Lett.* **101**, 107006 (2008).

³A. S. Sefat, R. Jin, M. A. McGuire, B. C. Sales, D. J. Singh, and D. Mandrus, *Phys. Rev. Lett.* **101**, 117004 (2008).

⁴Z. Ren, Q. Tao, S. Jiang, C. M. Feng, C. Wang, J. H. Dai, G. H. Cao, and Z. A. Xu, *Phys. Rev. Lett.* **102**, 137002 (2009).

⁵H. Okada, K. Igawa, H. Takahashi, Y. Kamihara, M. Hirano, H. Hosono, K. Matsubayashi, and Y. Uwatoko, *J. Phys. Soc. Jpn.* **77**, 113712 (2008).

⁶Z. A. Ren, W. Lu, J. Yang, W. Yi, X.-L. Shen, Z.-C. Li, G.-C. Che, X.-L. Dong, L.-L. Sun, F. Zhou, and Z.-X. Zhao, *Chin. Phys. Lett.* **25**, 2215 (2008).

⁷K. Miyazawa, K. Kihou, P. M. Shirage, C.-H. Lee, H. Kito, H. Eisaki, and A. Iyo, *J. Phys. Soc. Jpn.* **78**, 034712 (2009).

⁸Z. A. Ren, G. C. Che, X. L. Dong, J. Yang, Wei. Lu, W. Yi, X. L. Shen, Z. C. Li, L. L. Sun, F. Zhou, and Z. X. Zhao, *Europhys. Lett.* **83**, 17002 (2008).

⁹P. M. Shirage, K. Miyazawa, H. Kito, H. Eisaki, and A. Iyo, *Phys. Rev. B* **78**, 172503 (2008).

¹⁰J. Prakash, S. J. Singh, J. Ahmed, S. Patnaik, and A. K. Ganguli, *Physica C* **469**, 300 (2009).

¹¹J. Zhao, Q. Huang, C. de la Cruz, S. L. Li, J. W. Lynn, Y. Chen, M. A. Green, G. F. Chen, G. Li, Z. Li, J. L. Luo, N. L. Wang, and P. C. Dai, *Nat. Mater.* **7**, 953 (2008).

¹²C. H. Lee, A. Iyo, H. Eisaki, H. Kito, M. T. Fernandez-Diaz, T. Ito, K. Kihou, H. Matsuhata, M. Braden, and K. Yamada, *J. Phys. Soc. Jpn.* **77**, 083704 (2008).

¹³G. Garbarino, R. Weht, A. Sow, A. Sulpice, P. Toulemonde, M. Alvarez-Murga, P. Strobel, P. Bouvier, M. Mezouar, and M. Nunez-Regueiro, *Phys. Rev. B* **84**, 024510 (2011).

¹⁴G. Garbarino, R. Weht, A. Sow, C. Lacroix, A. Sulpice, M. Mezouar, X. Y. Zhu, F. Han, H. H. Wen, and M. Nunez-Regueiro, *Europhys. Lett.* **96**, 57002 (2011).

¹⁵S. A. Kimber, A. Kreyssig, Y.-Z. Zhang, H. H. Jeschke, R. Valentí, F. Yokaichiya, E. Colambier, J. Q. Yan, T. C. Hansen, T. Chatterji, R. J. McQueeney, P. C. Canfield, A. I. Goldman, and D. N. Argyriou, *Nat. Mater.* **8**, 471 (2009).

¹⁶K. Kuroki, H. Usui, S. Onari, R. Arita, and H. Aoki, *Phys. Rev. B* **79**, 224511 (2009).

- ¹⁷T. Saito, S. Onari, and H. Kontani, *Phys. Rev. B* **82**, 144510 (2010).
- ¹⁸I. Nishi, M. Ishikado, S. Ideta, W. Malaeb, T. Yoshida, A. Fujimori, Y. Kotani, M. Kubota, K. Ono, M. Yi, D. H. Lu, R. Moore, Z.-X. Shen, A. Iyo, K. Kihou, H. Kito, H. Eisaki, S. Shimoto, and R. Arita, *Phys. Rev. B* **84**, 014504 (2011).
- ¹⁹K. Miyazawa, S. Ishida, K. Kihou, P. M. Shirage, M. Nakajima, C. H. Lee, H. Kito, Y. Tomioka, T. Ito, H. Eisaki, H. Yamashita, H. Mukuda, K. Tokiwa, S. Uchida, and A. Iyo, *Appl. Phys. Lett.* **96**, 072514 (2010).
- ²⁰H. Yamashita, H. Mukuda, M. Yashima, S. Furukawa, Y. Kitaoka, K. Miyazawa, P. M. Shirage, H. Eisaki, and A. Iyo, *J. Phys. Soc. Jpn.* **79**, 103703 (2010).
- ²¹T. Hanna, Y. Muraba, S. Matsuishi, N. Igawa, K. Kodama, S.-I. Shimoto, and H. Hosono, *Phys. Rev. B* **84**, 024521 (2011).
- ²²S. Matsuishi, T. Hanna, Y. Muraba, S. W. Kim, J. E. Kim, M. Takata, S.-I. Shimoto, R. I. Smith, and H. Hosono, *Phys. Rev. B* **85**, 014514 (2012).
- ²³G. F. Chen, Z. Li, D. Wu, G. Li, W. Z. Hu, J. Dong, P. Zheng, J. L. Luo, and N. L. Wang, *Phys. Rev. Lett.* **100**, 247002 (2008).
- ²⁴H. Hiramatsu, T. Katase, T. Kamiya, M. Hirano, and H. Hosono, *Phys. Rev. B* **80**, 052501 (2009).
- ²⁵Y. Mizuguchi, K. Deguchi, S. Tsuda, T. Yamaguchi, and Y. Takano, *Phys. Rev. B* **81**, 214510 (2010).
- ²⁶I. Todorov, D. Y. Chung, H. Claus, C. D. Malliakas, A. Douvalis, and M. G. Kanatzidis, *Chem. Mater.* **22**, 3916 (2010).
- ²⁷H. Nakamura and M. Machida, *J. Phys. Soc. Jpn.* **80**, 073705 (2011).
- ²⁸Y. F. Guo, Y. G. Shi, S. Yu, A. A. Belik, K. Yamaura, and E. Takayama-Muromachi, *Physica C* **70**, S438 (2010).
- ²⁹Y. F. Guo, Y. G. Shi, S. Yu, A. A. Belik, Y. Matsushita, M. Tanaka, Y. Katsuya, K. Kobayashi, I. Nowik, I. Felner, V. P. S. Awana, K. Yamaura, and E. Takayama-Muromachi, *Phys. Rev. B* **82**, 054506 (2010).
- ³⁰M. Tanaka, Y. Katsuya, and A. Yamamoto, *Rev. Sci. Instrum.* **79**, 075106 (2008).
- ³¹F. Izumi and T. Ikeda, *Mater. Sci. Forum* **321–324**, 198 (2000).
- ³²Y. G. Shi, S. Yu, A. A. Belik, Y. Matsushita, M. Tanaka, Y. Katsuya, K. Kobayashi, Y. Hata, H. Yasuoka, K. Yamaura, and E. Takayama-Muromachi, *Phys. Rev. B* **80**, 104501 (2009).
- ³³A. Marcinkova, D. A. M. Grist, I. Margiolaki, T. C. Hansen, S. Margadonna, and Jan-Willem G. Bos, *Phys. Rev. B* **81**, 064511 (2010).
- ³⁴A. S. Sefat, R. Jin, M. A. McGuire, B. C. Sales, D. J. Singh, and D. Mandrus, *Phys. Rev. Lett.* **101**, 117004 (2008).
- ³⁵F. Han, X. Y. Zhu, P. Cheng, G. Mu, Y. Jia, L. Fang, Y. L. Wang, H. Q. Luo, B. Zeng, B. Shen, L. Shan, C. Ren, and H.-H. Wen, *Phys. Rev. B* **80**, 024506 (2009).
- ³⁶R. Pottgen and D. Johrendt, *Z. Naturforsch.* **63b**, 1135 (2008).
- ³⁷P. Popovich, A. V. Boris, O. V. Dolgov, A. A. Golubov, D. L. Sun, C. T. Lin, R. K. Kremer, and B. Keimer, *Phys. Rev. Lett.* **105**, 027003 (2010).
- ³⁸J. W. Stout and E. Catalano, *J. Chem. Phys.* **23**, 2013 (1955).
- ³⁹A. S. Sefat, A. Huq, M. A. McGuire, R. Jin, B. C. Sales, D. Mandrus, L. M. D. Cranswick, P. W. Stephens, and K. H. Stone, *Phys. Rev. B* **78**, 104505 (2008).
- ⁴⁰A. S. Sefat, M. A. McGuire, B. C. Sales, R. Jin, J. Y. Howe, and D. Mandrus, *Phys. Rev. B* **77**, 174503 (2008).
- ⁴¹C. Kittel, *Introduction to Solid State Physics*, 4th ed. (Wiley, New York, 1966).
- ⁴²J. Karpinski, N. D. Zhigadlo, S. Katrych, Z. Bukowski, P. Moll, S. Weyeneth, H. Keller, R. Puzniak, M. Tortello, D. Daghero, R. Gonnelli, I. Maggio-Aprile, Y. Fasano, Ø. Fischer, K. Rogacki, and B. Batlogg, *Physica C* **469**, 370 (2009).
- ⁴³U. Welp, W. K. Kwok, G. W. Crabtree, K. G. Vandervoort, and J. Z. Liu, *Phys. Rev. Lett.* **62**, 1908 (1989).
- ⁴⁴P. Fournier and R. L. Greene, *Phys. Rev. B* **68**, 094507 (2003).
- ⁴⁵I. W. Sumarlin, S. Skanthakumar, J. W. Lynn, J. L. Peng, Z. Y. Li, W. Jiang, and R. L. Greene, *Phys. Rev. Lett.* **68**, 2228 (1992).
- ⁴⁶S. I. Vedenev, A. G. M. Jansen, E. Haanappel, and P. Wyder, *Phys. Rev. B* **60**, 12467 (1999).
- ⁴⁷N. R. Werthamer, E. Helfand, and P. C. Hohenberg, *Phys. Rev.* **147**, 295 (1966).
- ⁴⁸D. Berardan, L. D. Zhao, L. Pinsard-Gaudart, and N. Dragoe, *Phys. Rev. B* **81**, 094506 (2010).
- ⁴⁹F. Hunte, J. Jaroszynski, A. Gurevich, D. C. Larbalestier, R. Jin, A. S. Sefat, M. A. McGuire, B. C. Sales, D. K. Christen, and D. Mandrus, *Nature (London)* **453**, 903 (2008).
- ⁵⁰G. F. Chen, Z. Li, G. Li, J. Zhou, D. Wu, J. Dong, W. Z. Hu, P. Zheng, Z. J. Chen, H. Q. Yuan, J. Singleton, J. L. Luo, and N. L. Wang, *Phys. Rev. Lett.* **101**, 057007 (2008).
- ⁵¹J. P. Carbotte, *Rev. Mod. Phys.* **62**, 1027 (1990).
- ⁵²C. P. Bean, *Rev. Mod. Phys.* **36**, 31 (1964).
- ⁵³M. Putti *et al.*, *Supercond. Sci. Technol.* **23**, 034003 (2010).
- ⁵⁴S. Lee *et al.*, *Appl. Phys. Lett.* **95**, 212505 (2009).
- ⁵⁵J. Ju, K. Huynh, J. Tanga, Z. F. Lia, M. Watahikia, K. Satoa, H. Terasakib, E. Ohtanib, H. Takizawac, and K. Tanigakia, *J. Phys. Chem. Solids* **71**, 491 (2010).
- ⁵⁶G. Garbarino, P. Toulemonde, M. Alvarez-Murga, A. Sow, M. Mezouar, and M. Nunez-Regueiro, *Phys. Rev. B* **78**, 100507(R) (2008).
- ⁵⁷P. M. Shirage, K. Miyazawa, K. Kihou, H. Kito, Y. Yoshida, Y. Tanaka, H. Eisaki, and A. Iyo, *Phys. Rev. Lett.* **105**, 037004 (2010).